

# Fluid Flow Modeling in a Gas-Filled Optical Cell

S. Boutebba, W. Kaabar and R. Hadjadj

Département de Chimie, Faculté des Sciences Exactes, Université Mentouri, Constantine 25000, Algeria  
E-mail: bouteb.souha@yahoo.fr

**Abstract:** This paper presents a modelling investigation of the recirculating nitrogen gas flows present in an optical cell containing an incandescent filament. The free convective fluid flows are driven by the hot filament located centrally in the cylindrical cell; gas temperatures range from 380 K in wall regions to 2700 K at the filament. The fluid physical properties are temperature dependent. The model equations of continuity, Navier-Stokes and energy are numerically solved with a finite volume method. The obtained results show that the thermal and velocity fields have three-dimensional flow characters. Strong convective effects are observed around the filament ends, where the highest temperature gradients are found. The study demonstrates the end effects on the temperature distribution and fluid flow.

**Keywords:** heat transfer, fluid flow, convection, temperature distribution, CFD.

## 1. Introduction

Early models of the flow within gas filled incandescent light sources hypothesized a thin stagnant conduction dominated layer surrounding the filament, within which the transition from filament to wall temperature occurred [1, 2]. These models provide reasonable estimates of gross heat transfer for power balance calculations [3], but are insensitive to orientation and geometry. Most importantly, they do not account for convective flows in the gas filling. The complete flow field is obtained through solution of the Navier-Stokes equations which describe the conservation of energy, momentum and mass. Fisher and Fitzgerald [4] solved the conservation equations in two dimensions and successfully predicted the flow patterns and tungsten transport in horizontal cylindrical lamps. The calculated temperature profiles showed good agreement with those obtained from a double exposure holographic technique. It was also demonstrated that lower gas filling pressures reduced the magnitude of convective effects. Correa [5] calculated the fluid flow and heat transfer inside tungsten halogen lamps using an advanced curvilinear body fitted calculation grid. Flow patterns were simulated for vertically and horizontally orientated lamps containing an inert gas at high pressure. Recently, Makai et al. [6] developed a computer model to evaluate the operating conditions in tungsten halogen lamps based on the substantial partial differential equations of the free convection problem. The free convection was simulated by the convection-conduction equation and the incompressible Navier-Stokes equation. They determined the temperature distribution, the velocity field and the pressure in these lamps. The pressure dependence on dimensionless characteristic numbers was evaluated. Different least square estimation methods for determination of distribution temperature and their applicability with regard to uncertainties of the spectral irradiance data of incandescent lamps were discussed by Rosenkranz et al. [7].

In the present paper we consider a numerical study of convection in a cylindrical cell subjected to a temperature gradient. Gas temperatures range from 380 K in wall regions to 2700 K at the filament; gas temperature gradients of over  $500 \text{ K mm}^{-1}$  exist near the filament. The flow is driven by the thermal buoyancy. This work was carried out using the general purpose fluid dynamic computer code, Fluent [8]. Fluent is a state of the art CFD (Computational Fluid Dynamics) computer package for modelling fluid flow and heat transfer problems in complex geometries. This program originates from work described by Patankar [9].

## 2. Problem definition

The subject of the investigations is a high temperature cell. The optical cell is assumed to be a long cylinder with an axial tungsten filament having no velocity or temperature gradients along the cylinder axis. The cylindrical shape of the cell will allow for symmetry simplifications in the theoretical modeling. The cell envelope is defined to be 75 mm in diameter and 250 mm in length. The filament is modeled as a solid cylinder with a diameter of 1.58 mm and a length of 23.5 mm. Boundary conditions are set equal to 2700 K for the filament and 380 K for the lamp envelop. A cold filling pressure (31596 Pascal) is used to maintain significant buoyancy driven gas flows in the cell whilst preventing wall blackening by tungsten deposition. The physical system we consider is nitrogen gas in local thermodynamic equilibrium at all points in the flows. Nitrogen gas filling is required because it has favorable thermal conductivity properties and has little tendency to arc.

Physical constants relevant to the case under study include the operating pressure, density, heat capacity and transport properties of the fluid. The transport properties (viscosity and thermal conductivity) and the heat capacity are specified as temperature dependent polynomials.

In the present investigation, the data of Svehla [10] is used to generate the best fit polynomials. Transport property polynomials for pure nitrogen are used in all calculations.

We have, firstly, used a two dimensional model (2D) for the investigation of the interior of the optical cell and then extended the model to include a full three dimensional simulation (3D).

### 3. Numerical procedure

The flow and heat transfer phenomena to be investigated here are basically described by the equations of continuity, Navier-Stokes and energy. The fluid is regarded as Newtonian and incompressible; the flow is laminar in steady regime. Radiation heat transfer is negligible.

For this work a non-uniform grid consisting of tetrahedral elements is used. Once the grid has been created, the governing equations of conservation of mass, momentum and energy are solved in each cell. This results in a set of simultaneous algebraic equations for all elements, which is solved through a finite volume method. A second order upwind discretisation is used to calculate the fluxes in the discretised equations. The resulting of algebraic equations has been solved using the iterative line-by-line method associated with the tri-diagonal matrix algorithm (TDMA). This starts from a set of arbitrary initial conditions (except for at the boundaries) and converges to the correct solution after a number of iterations. Coupled velocity-pressure calculations have been performed using the SIMPLE algorithm. Convergence is considered to be reached when the normalized residuals have fallen below  $10^{-4}$ . An exception to this general value is that taken for the enthalpy residual, for which a value of  $10^{-6}$  is more appropriate. Velocity and temperature fields are obtained.

## 4. Results and Discussion

### 4.1. A two dimensional model

Initial model is based upon a 2D model of the lamp. A semi-circular (exploiting the vertical symmetry plane of the lamp) and a non-uniform grid, where a greater number of cells are concentrated in the regions expected to contain steep gradients of flow variables, is constructed with 20000 nodal points on the basis of many tests. This computational grid is illustrated in Fig. 1.

Using the temperature distribution in the vertical plane, a grid sensitivity study has been conducted. Five numerical grids have been used to estimate the effect of the grid resolution on the results (Fig. 2). It is found that the grids with 27528 nodes and 20000 nodes give similar results and so the latter mesh is used throughout this study.

The problem case described above is then submitted for computation and a converged solution is obtained after performing 3000 iterations. Fig. 3 shows the calculated velocity and temperature fields when the optical cell is viewed along the longitudinal axis of the filament.

The velocity field exhibits recirculation patterns of free convection around a heated cylinder in an enclosure [11], the flow shows the buoyant plume. The maximum gas velocity is equal to 0.275 m/s and occurs at about 1 cm to the side of the filament, indicating that significant convective currents do occur within the gas filling. Very steep temperature gradients are seen to exist in the filament region particularly below the filament where the temperature field is somewhat compressed by the flow pattern. The temperature contours are distorted by the convective flows from the purely radial dependence found for the case where the heat transfer is based only on conduction, indicated by a series of concentric circles. The mixing of cooler gas into the hot filament region accounts for the generally lower temperatures which imply less viscous flows and somewhat higher velocities.

Between the heated filament and the upper side of the lamp the thermal stratification is instable: the relatively cold fluid near the upper envelope is denser than the hot fluid next to the filament. This instable thermal stratification induces an upward fluid motion from the filament towards the lamp upper surface. This flow is therefore induced by the buoyancy effect. Once the flow reaches the upper envelope, it is diverted by the lamp surface, and follows a circular motion towards the bottom part of the lamp. At this location, the flow is induced upward towards the filament. This fluid motion generates two counter rotating vortices, separated by the vertical plane of symmetry.

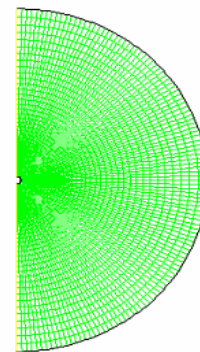


Figure 1. 2D computational grid

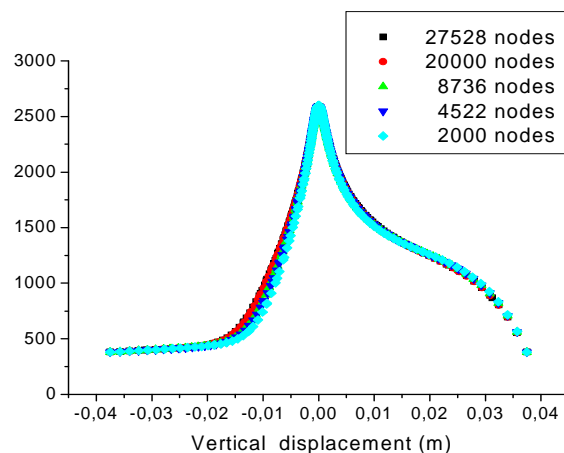


Figure 2. Sensitivity to mesh density

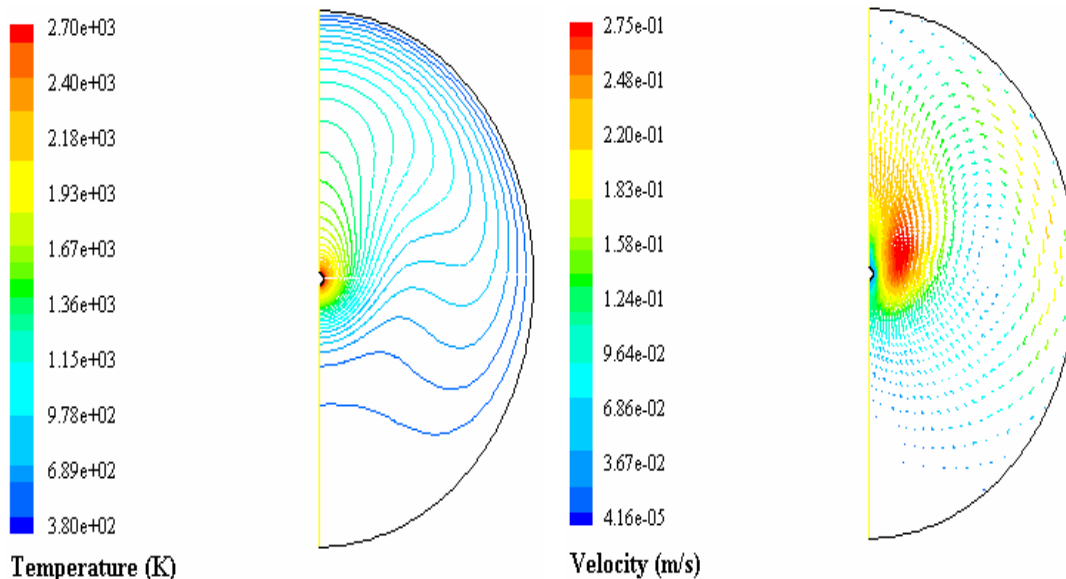


Figure 3. Temperature contours and velocity vectors

4.2. A three dimensional model

Clearly the length of the filament is not equal to that of the lamp envelope, this, results in a fairly large volume of cooler gas at the lamp sides which lead to a lower mean temperature in the system. Furthermore, the temperature along the filament is not constant but decreases from its centre to its extremities. The 2D investigation is being refined and extended to account for 3D effects.

The lamp geometry in three dimensions is defined exploiting the symmetry of the device. Two vertical symmetry planes, one containing the filament axis and the other perpendicular to the filament and passing through its centre, are encountered. This reduces the computational domain to the quarter of the total lamp volume. A non-uniform grid (Fig. 4) is used with the highest grid density in the regions where the steepest physical property gradients are envisaged. There are in the filament region in the axial direction, and close both to the filament and to the lamp envelope in the radial direction.

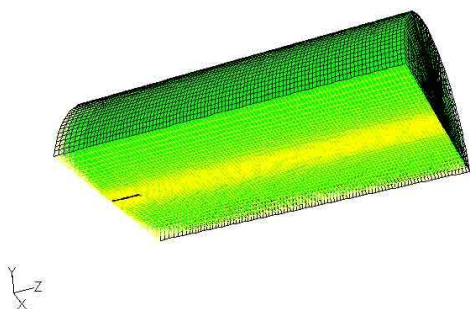


Figure 4. 3D computational grid

Fig. 5 shows a comparison of the temperature field in the plane perpendicular to the filament mid-point for both the 2D and 3D cases. It can be seen that both models

exhibit similar features, however the temperature distribution is more compressed in the 3D model.

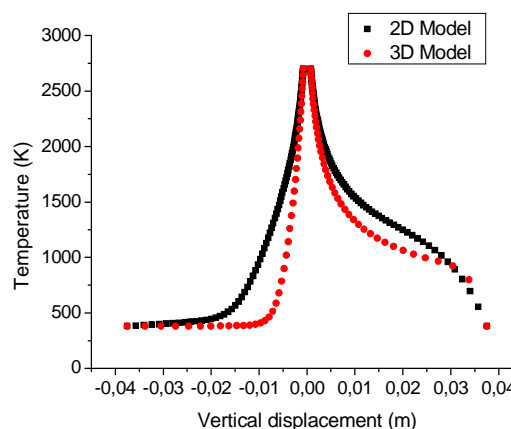


Figure 5. Temperature fields for the 2D and 3D models

Features of the 3D results for the velocity and temperature fields are presented in Figures 6, 7 and 8.

The principal feature of the velocity has, as in 2D investigation, a vortex structure in planes perpendicular to the filament axis. The magnitudes of the velocity decrease on moving from the filament's mid-point to the lamps end wall. The axial components of the velocity cause a mixing of cooler gas from the lamp end into the hot filament region. This cooling effect accounts for generally lower temperatures being predicted than in the 2D case. Lower temperatures mean a correspondingly less viscous system and hence higher average velocities. The maximum velocity is predicted to be in the plane perpendicular to the filament mid-position with magnitude equal to 0.61 m/s as opposed to a value of 0.275 m/s in the corresponding 2D case. Furthermore, in the plane perpendicular to the filament's mid-point, the recirculation pattern is more

compact than in the 2D case and the maximum velocity is no longer observed to the side of the filament but is situated now about 0.5 cm above the filament. This is a consequence to the lower mean temperature which results in a higher Rayleigh number and thus to stronger convection effects.

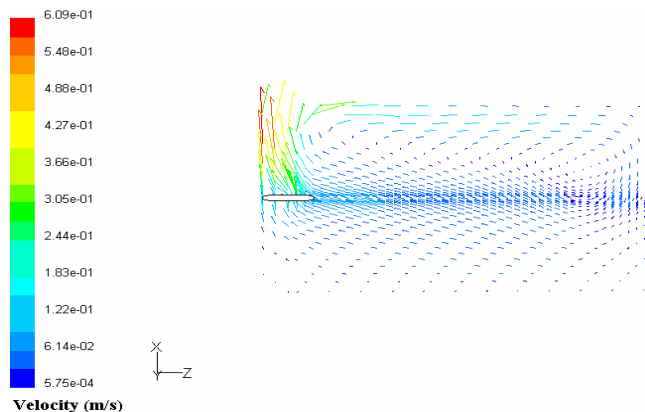


Figure 6. Velocity vectors in the vertical plane containing the filament axis

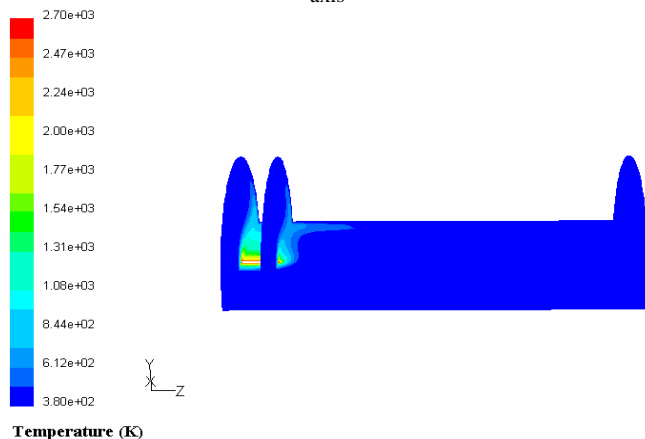


Figure 7. Temperature distribution in planes perpendicular to the filament axis

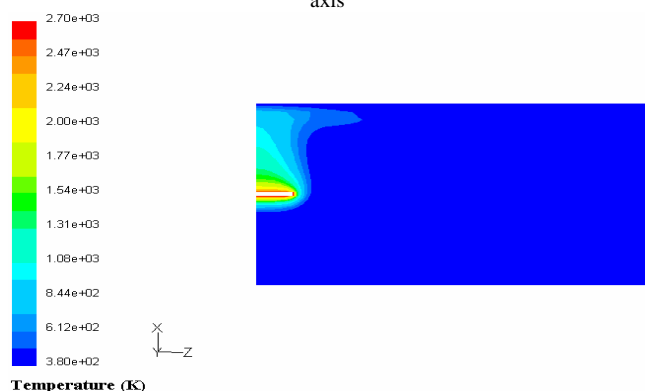


Figure 8. Temperature distribution in the vertical plane containing the filament axis

Fig. 7 shows temperature distribution in planes perpendicular to the filament axis. It can be seen that convection effects are more important than in the corresponding 2D case due to the increase of the Rayleigh number by 3D effects. Furthermore as one moves away

from the filament centre toward the lamp's end wall, convection effects become less important until an almost stagnant gas region at the lamp's end wall is reached.

Fig. 8 shows the distribution of the temperature in the vertical plane containing the filament axis. It is shown that in the filament mid-point region, contours nearly parallel to the filament are observed, meaning that, in this region, axial temperature gradients are close to zero.

These figures clearly show the strongly three dimensional nature of the flow patterns. Earlier experimental studies of such lamps [12, 13] found that the highest wall deposition rates occurred around the filament ends, this would be expected from the flow patterns predicted here as the increased gas flows in such positions cause an enhanced tungsten transport in these regions.

The numerical results of our study are in good agreement with those of an experimental and theoretical work done with the same geometric, dynamic and thermal parameters [13].

## 5. Conclusions

The study presented here has shown that the 2D investigation gives generally a good account of the magnitude and spatial distribution of the temperature and the velocity. 3D effects however are found to lead to more compressed features in both the temperature and the velocity due to the higher Rayleigh number. The highest flow velocities occur around the filament ends, where the highest temperature gradients are found.

The present results are of relevance to spectroscopic measurements of temperature based on  $N_2$ , including coherent anti-Stokes Raman scattering thermometry.

## REFERENCES

1. Langmuir I., *Phys. Rev.*, 34, **1912**, 401-422.
2. Elenbass W., *J. Appl. Phys.*, 19, **1948**, 1148-1154.
3. Howe S.H., *Proc. of North America Illuminating Engineering Society*, paper 13, **1982**.
4. Fisher E. and Fitzgerald J., *J. Appl. Phys.*, 45, **1974**, 2895-2902.
5. Correa S.M., *Int. J. of Heat and Mass Trans.*, 30, **1987**, 663-672.
6. Makai L., Hárs G., Varga G. and Deák P., *J. Phys. D: Appl. Phys.*, 38, **2005**, 3217-3225.
7. Rosenkranz P., Matus M. and Rastello M.L., *Metrologia*, 43, **2006**, 130-134.
8. Fluent. Inc., *Fluent documentation*, www.fluent.com, **2006**.
9. Patankar S.V., *Numerical Heat Transfer and Fluid Flow*, McGraw-Hill, **1980**.
10. Svehla R.A., *NASA Tech. Rep.*, R-132, **1962**.
11. Farouk B. and Guceri S.I., *Int. J. Heat and Mass Transfer*, 26, **1983**, 231-243.
12. Schnedler E., *High. Temp. Sci.*, 19, **1985**, 237-242.
13. Devonshire R., Dring I.S., Hoey G., Porter F.M., Williams D.R. and Greenhalgh D.A., *Chem. Phys. Lett.*, 129, **1986**, 191-196.

Received: 07 October 2011

Accepted: 28 December 2011